ARKIV FÖR FYSIK Band 18 nr 4

Communicated 27 January 1960 by O. KLEIN and I. WALLER

A solid state *spd*-MOLCAO treatment of cubic-octahedral CaB_6 with variation of the *d* orbital exponent

By S. FLODMARK

With 4 figures in the text

SUMMARY

The present work is a direct continuation of an earlier investigation by the author on the same subject [1]. The question of finiteness for the energy per unit cell of the crystal has been discussed. A numerical mistake, which, however, does not change the main qualitative conclusions made in [1], has been corrected. The energy bands have been computed for five different choices of the *d* orbital exponent. The result of these new calculations indicates that a remarkable increase in the *d* orbital exponent, when chosen according to the Slater rules, is required to minimize the energy.

Introduction

The metal borides of type MB_6 have earlier been investigated experimentally by Kiessling [2] and theoretically by the present author [1, 3, 4] and by Longuet-Higgins and de Roberts [5]. In the present investigation the secular equations for the different symmetry adapted orbitals of the B_6 valence electrons are solved in the *spd* approximation with variable *d* orbital exponent.

Section 1 gives the effective Hamiltonian operator for an electron in the average field of the rest of the crystal. The total Hamiltonian operator of the system considered has been given and divided up into equal parts comparable to the effective operator. It turns out that both operators are finite and have the same order of magnitude. Section 2 gives the numerical results of the present calculations including variations of the *d* orbital exponent. The existence of conduction bands and the great influence of *M* shell orbitals strongly dependent on their orbital exponents, is verified.

The effective Hamiltonian operator of CaB_6[1]

We denote the valence electrons by i or j, the boron nulei (nuclei + inner electrons) by B_0 or B and the ionized Ca atoms (considered as point charges) by M_0 or M (metal). The total Hamiltonian operator for the system under consideration is given by eq. (37) of [1]:

---

[1] Before discussing the Hamiltonian operator it may be convenient to correct some misprints occurring in [1]:

p. 530, eq. (37). A factor 2 is missing for the term $\sum_i^{(B_0)} 1/r_{iB}$. (The notation B_0 here stands for the nucleus "belonging to" the electron i).

$$H=\sum_i\left(-\frac{1}{2}\Delta_i-\sum_B\frac{Z_B}{r_{iB}}-\sum_M\frac{Z_M}{r_{iM}}\right)+\frac{1}{2}\sum_i\sum_{j\neq i}\frac{1}{r_{ij}}+\frac{1}{2}\sum_{B_0}\sum_{B\neq B_0}\frac{Z_B Z_{B_0}}{r_{BB_0}}+$$

$$+\frac{1}{2}\sum_{M_0}\sum_{M\neq M_0}\frac{Z_M Z_{M_0}}{r_{MM_0}}+\sum_B\sum_M\frac{Z_B Z_M}{r_{BM}}+E_I. \tag{1}$$

The constant nuclear energy in the second line of (1) must be added to get a finite crystal energy per unit volume. This also implies that the cohesive energy with opposite sign is given by (1). The nuclear charges are

$$Z_B=Z_{B_0}=3;\ Z_M=Z_{M_0}=2\lambda, \tag{2}$$

where $\lambda=1$ for complete ionization of Ca.

Our intention is now to split the Hamiltonian operator (1) into an infinite sum of identical formal one-electron operators. We denote by h_0 the Hamiltonian operator of one electron in the field of all the nuclei:

$$h_0=-\frac{1}{2}\Delta-\sum_B\frac{Z_B}{r_B}-\sum_M\frac{Z_M}{r_M}. \tag{3}$$

The potential energy part of (3) tends towards infinity for an infinite crystal, since the number of atom neighbours at a certain distance is proportional to the squared atomic distance.

The coulomb interaction energy between one electron and all the others may be written

$$h_e=\sum_{i\neq 1}\frac{1}{r_{1i}}. \tag{4}$$

The nuclear B-B interaction energy for one boron atom divided by the average number of valence electrons per boron atom,

$$n_B=Z_B+Z_M/6=3+\lambda/3, \tag{5}$$

can be written

$$\varepsilon_B=\frac{Z_B}{Z_B+Z_M/6}\sum_{B\neq B_0}\frac{1}{r_{BB_0}}=\frac{3}{1+\lambda/9}\sum_B. \tag{6}$$

Here we have introduced the notation

---

p. 531, eq. (38). A factor λ is missing for the term $\sum_M^{(8)} 2/r_{MB_0}$.

p. 535, eq. (48). The term, $\bar{Z}_b/R_b$ must be replaced by Z_b/R_b. The sign of the term containing $\sum_{b'}^{(24)}$ must be changed.

$$\sum_B = \sum_B \frac{1}{r_{BB_0}}. \tag{7}$$

This term is also infinite. Similarly, we can introduce the nuclear M-M interaction energy "per valence electron"

$$\varepsilon_M = \frac{Z_M^2}{6\,Z_B + Z_M} \sum_M \frac{1}{r_{MM_0}} = \frac{2\,\lambda^2}{9+\lambda} \sum_M \frac{1}{r_{MM_0}} = \frac{2\,\lambda^2}{9+\lambda}\,\frac{1}{6} \sum_B + \beta, \tag{8}$$

where β is a finite positive constant with a definite value for $\lambda = 1$ ($\beta \approx 0.2$ a.u.). The electron-electron energy (4) can also be expressed by use of (7):

$$h_e = (3 + \lambda/3) \sum_B + \delta, \tag{9}$$

where δ is a finite operator with expectation values determined essentially by the electronic interaction between one valence electron and all the other valence electrons within the same boron atom (order of magnitude $\delta \sim 0.6$ a.u.).

Furthermore we introduce the average nuclear B-M interaction energy per electron,

$$\varepsilon_{BM} = \frac{Z_B\,Z_M}{Z_B + Z_M/6} \sum_M \frac{1}{r_{BM}} = \frac{2\,\lambda}{1+\lambda/9} \sum_M \frac{1}{r_{BM}}. \tag{10}$$

Finally the ionization energy, E_I, may be taken per electron, yielding

$$\varepsilon_I = \frac{I}{18 + 2\,\lambda}, \tag{11}$$

where I is the ionization energy of one Ca atom.

The total Hamiltonian operator (1) "per electron" may then be written by using (3), (4), (6), (8), (10) and (11) as a formal "one-electron operator":

$$h_1 = h_0 + \tfrac{1}{2}\,h_e + \tfrac{1}{2}\,\varepsilon_B + \tfrac{1}{2}\,\varepsilon_M + \varepsilon_{BM} + \varepsilon_I. \tag{12}$$

Since, however, h_e in fact is a two-electron operator, (12) cannot be used as an effective one-electron Hamiltonian operator. To construct such an effective operator, we must compensate for the electron-electron interaction by using effective charges, Z_B^{eff}, chosen differently for different atomic distances and different atomic orbitals involved in the integrals occurring for the energy expectation values (see [1], Table 6).

The effective Hamiltonian operator used for the energy band calculations in [1] is given by [1], (38):

$$h = -\frac{1}{2}\Delta - \sum_B \frac{Z_B^{\text{eff}}}{r_B} - \sum_M \frac{2\,\lambda}{r_M} + \frac{1}{1+\lambda/9}\left(\sum_B \frac{Z_B^{\text{eff}}}{r_{BB_0}} + \sum_M \frac{Z_B^{\text{eff}}}{r_{BB_0}} + \sum_M \frac{2}{r_{MB_0}}\right) + \varepsilon_I. \tag{13}$$

The first three terms of (13) are dependent on the atomic orbitals involved. Here, Z_B^{eff} is chosen to satisfy the relation

$$-\frac{1}{2}\Delta-\sum_{B}\frac{Z_B^{\text{eff}}}{r_B}-\sum_{M}\frac{2\lambda}{r_M}\sim h_0+h_e \tag{14}$$

as well as possible. The nuclear energy in (13) added to this quantity in order to get a finite energy, is the interaction energy between one boron nucleus and all the other atoms per electron. Since the valence electrons shield the boron nuclei, effective charges occur also here. These effective charges tend indefinitely towards $Z^{\text{eff}}=-\lambda/3$ for large distances. Consequently we have a relation similar to (6):

$$\varepsilon_B^{\text{eff}}=\frac{1}{1+\lambda/9}\sum_{B}\frac{Z_B^{\text{eff}}}{r_{BB_0}}=-\frac{\lambda/3}{1+\lambda/9}\sum_{B}+\alpha, \tag{15}$$

where α has a small finite value ($\alpha=0.02$ a.u. for $\lambda=1$).

Using the equations (14), (15) and (10) we can write (13):

$$h\sim h_0+h_e+\varepsilon_B^{\text{eff}}+\varepsilon_{BM}+\varepsilon_I. \tag{16}$$

Since the effective charges tend towards $-\lambda/3$, the sums for large distances can be calculated as pure Madelung energies. As is well known, these energies are convergent under the condition that the terms are added in suitable sequence of neutrally charged groups [6].

Let us now consider the difference between (16) and (12):

$$h-h_1\sim\tfrac{1}{2}h_e+\varepsilon_B^{\text{eff}}-\tfrac{1}{2}\varepsilon_B-\tfrac{1}{2}\varepsilon_M. \tag{17}$$

Inserting into (17) the relations (9), (15), (6) and (8), we find that the coefficient of $\sum_B$ vanishes identically, giving a finite difference

$$h-h_1\sim\alpha+\tfrac{1}{2}(\delta-\beta)\sim 0.2 \text{ a.u.} \tag{18}$$

Thus both h_1 and h are finite and their expectation values have the same order of magnitude.

The effective Hamiltonian operator (13) has been used for determining the energy bands. The sums over neighbouring atoms have been performed for the 24 nearest boron atoms and the 8 nearest metal atoms. The remaining terms have been summed up as electrostatic point charge interaction (Madelung energy) and put in the last term of [1], (38). The notation ε_R is used for this quantity per B_6 octahedron.

The quantities (47) and (48) of [1] entering in the secular equations, which give the energy bands corresponding to (13), can be written (with the approximations and notations introduced in [1]):

$$h_0=\langle B_0|h|B_0\rangle=C_0-Z_0B_0-\sum_{b}^{(24)}Z_b\left(D_b-\frac{A_0}{R_b}\right)-\sum_{m}^{(8)}2\lambda\left(D_m-\frac{A_0}{R_m}\right)+\varepsilon_0A_0; \tag{19}$$

$$h_b=C_b-\bar{Z}_bB_b+\frac{Z_b}{R_b}A_b+\varepsilon_0A_b, \tag{20}$$

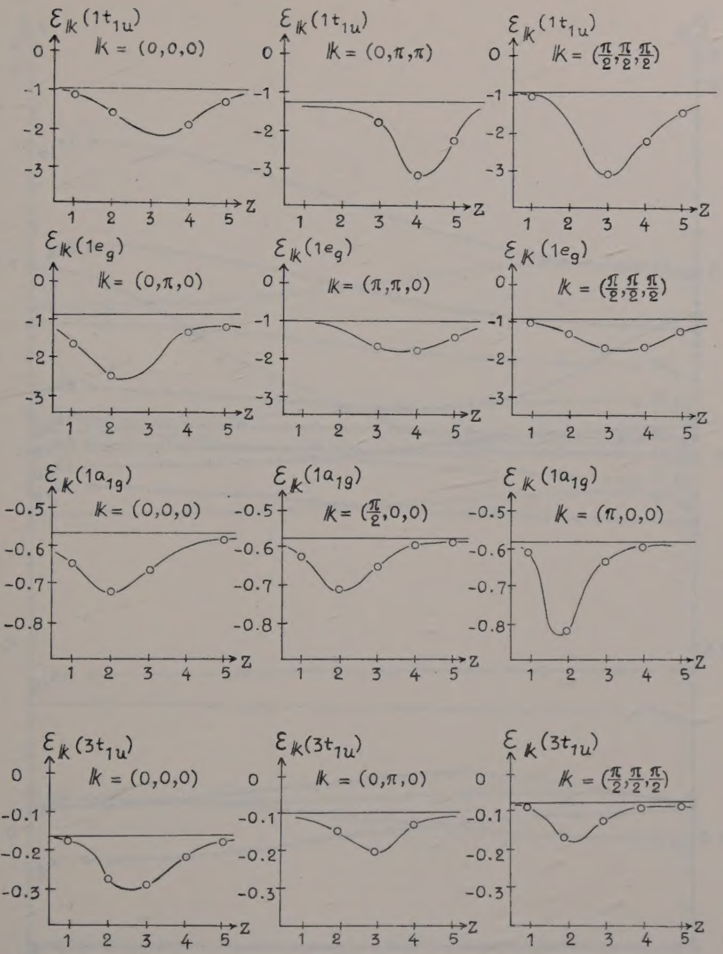

Fig. 1. Energy eigenvalues, $\varepsilon_{\mathbf{k}}$, given in a.u. for the bonding orbitals for some different **wave** vectors in the *LM* approximation as functions of the *d* orbital exponent $Z/3$. The straight lines correspond to the *L* approximation.

where ε_0 is a constant not depending on the special orbitals involved:

$$\varepsilon_0 = \frac{1}{18+2\lambda}\left\{I + \lambda^2 \varepsilon_R - 2\lambda\left(\sum_b^{(24)} \frac{Z_b}{R_b} + \sum_m^{(8)} \frac{2\lambda}{R_m}\right)\right\}. \tag{21}$$

For complete ionization ($\lambda = 1$), $\varepsilon_0 = -0.059$ a.u. The negative sign of this quantity indicates that the stability of the crystal is somewhat increased on account of ionization.

In determining the one-electron crystal energy we have not compared it to the mean binding energy of an electron in a free boron atom, which, however, might be more realistic than to compare it to a state where all the considered particles are free. Thus this binding energy term should also be added, increasing

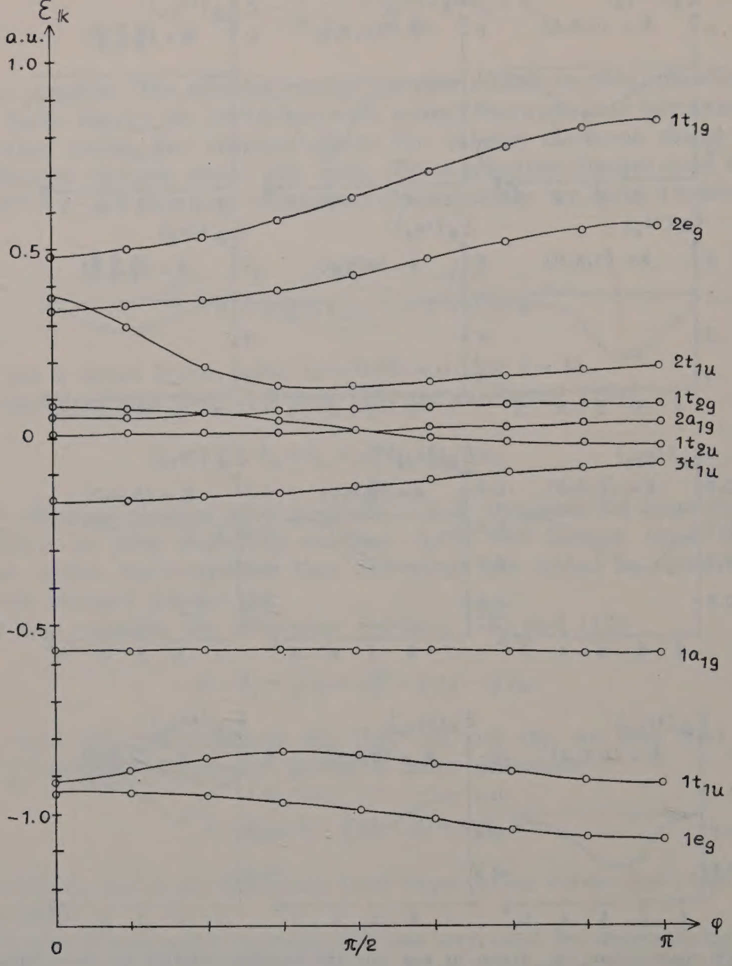

Fig. 2 a. Energy bands $\varepsilon_{\mathbf{k}}$ in the L approximation. $\mathbf{k} = (\varphi, 0, 0)$.

the orbital energies somewhat. This might be taken into account by increasing the constant term ε_0.

The energy bands given in section 2 have been calculated, for simplicity, by putting $\varepsilon_0 = 0$. To get the actual bands corresponding to (13), the given bands thus ought merely to be lowered by the quantity 0.059 a.u. But, since the zero point level cannot be meaningfully defined with very great accuracy, this common lowering of the bands has no certain importance and can be neglected.

Unfortunately, the mistake of sign in [1, (48)] also appeared in the numerical calculations, but renewed calculations show that the main qualitative conclusions still hold. In addition to these calculations variation has been performed for the *d* orbital exponents, the result of which will be given in section 2.

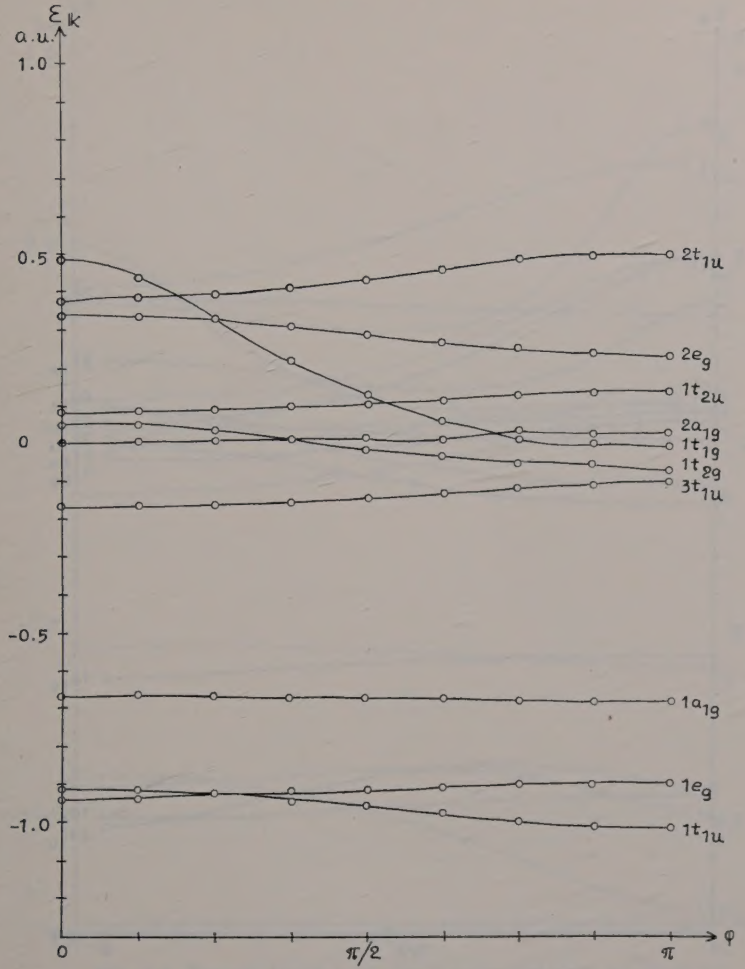

Fig. 2 b. Energy bands $\varepsilon_{\mathbf{k}}$ in the L approximation. $\mathbf{k} = (0, \varphi, 0)$ and $(0, 0, \varphi)$.

2. Electron distribution and energy bands for different *d* orbital exponents

The molecular integrals occurring in (19) and (20) have been calculated by means of a programme, made by the present author, for the electronic computer Besk [7]. This programme is free for anyone to use and a special table computed by use of it can be bought [8]. Also the different secular equations have been solved by means of Besk.

The electron distribution and the energy bands were given in [1] in the L approximation (including hybrids of $2s$ and $2p$ orbitals) and in the LM approximation (including hybrids of $2s$, $2p$, $3s$, $3p$ and $3d$ orbitals). The L shell orbital exponents were chosen according to Duncanson and Coulson [9]. For the M shell, the orbital exponents were chosen according to Slater's rule, yielding the effective charge $Z=1$.

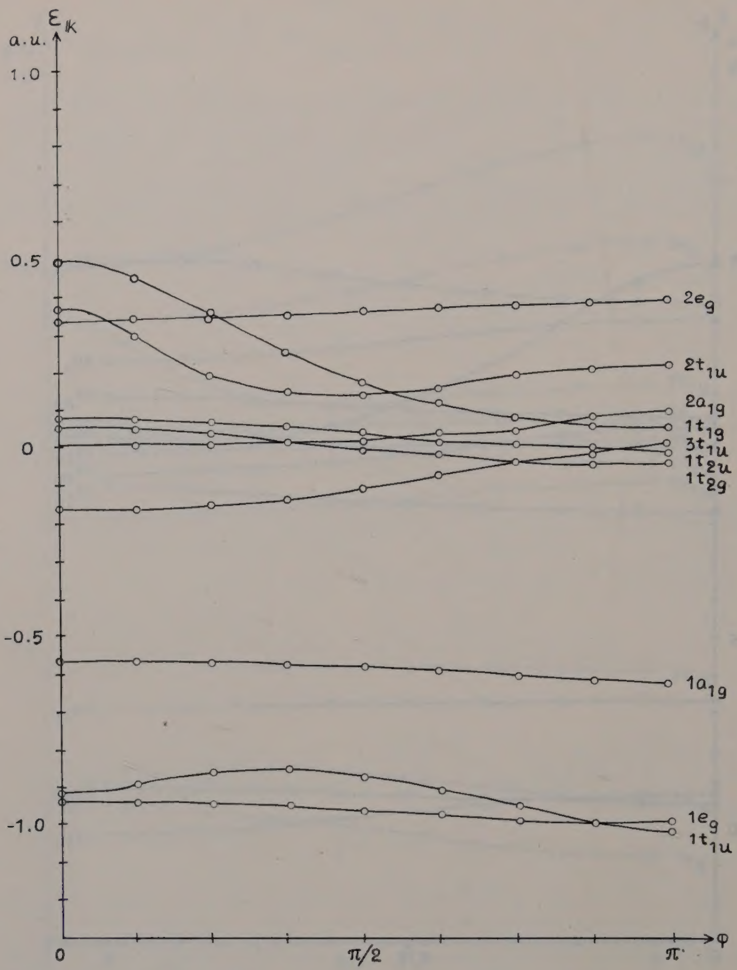

Fig. 2 c. Energy bands $\varepsilon_{\mathbf{k}}$ in the L approximation. $\mathbf{k} = (\varphi, \varphi, 0)$ and $(\varphi, 0, \varphi)$.

The overlap between M shell orbitals of neighbouring atoms is, however, very great, indicating that the orbital exponents should rather be chosen according to the conditions in the whole crystal than in the free atom. This great overlap also causes great overlap elements for the corresponding crystal orbitals occurring in the secular equations. Thus the eigenvalues and eigenvectors are very sensitive to small changes in the secular elements. Moreover, very many neighbours must be taken into consideration on account of the long range interaction for M shell orbitals with small orbital exponents. Since it would lead to quite extensive calculations to take sufficiently many neighbours into account, some of the secular overlap matrices are indefinite in the present approximation.

An increase of the effective charge of the M shell orbitals to about $Z = 5$ would, however, decrease the interaction range for these orbitals to the same order of

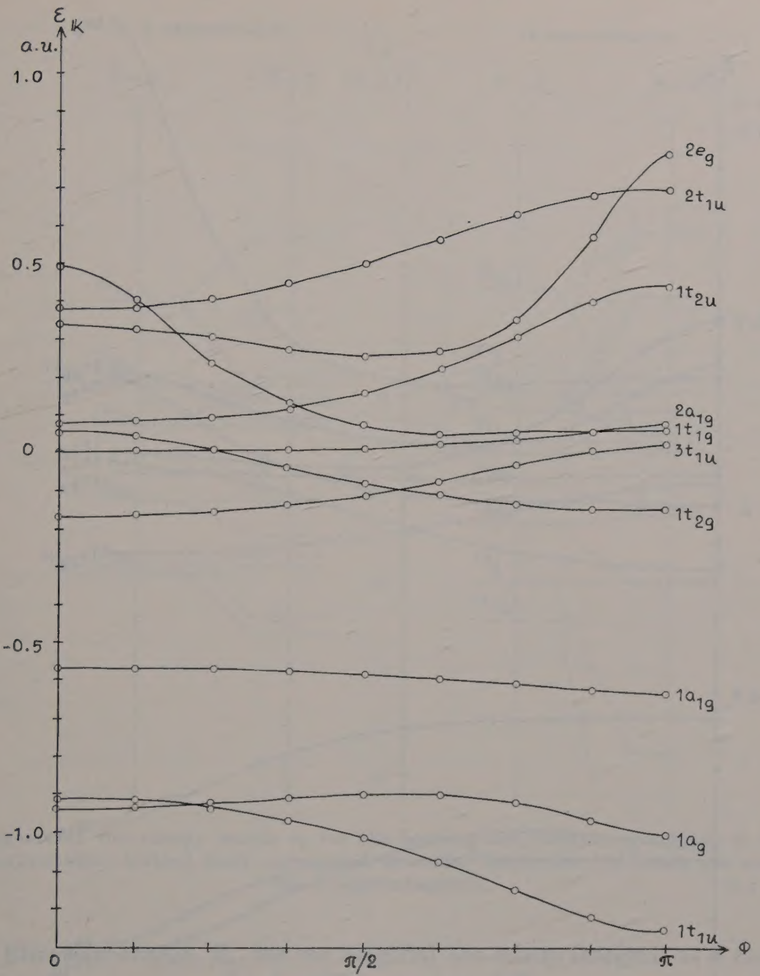

Fig. 2 d. Energy bands $\varepsilon_{\mathbf{k}}$ in the L approximation. $\mathbf{k} = (0, \varphi, \varphi)$.

magnitude as for the L shell orbitals (cf. [7], Figs. 2, 3 and 4). The secular equations corresponding to the interrupted series of neighbours in the atomic integrals (cf. (19)) has consequently in general no indefinite overlap matrices. For somewhat smaller choice of Z, however, some of the overlap matrices are indefinite, or nearly so, and the corresponding secular equations cannot be solved without taking many more neighbours into account.

Since $2s$ and $3s$ orbitals are only slightly different, when the orbital exponents are chosen to give nearly equal interaction range, *i.e.* the overlap between normalized crystal orbitals constructed from $2s$ and $3s$ orbitals tends towards 1, corresponding to a "nearly indefinite" metric, it gives very little extra information to make use of both. The same thing is valid for parallel $2p$ and $3p$ orbitals. Thus $3s$ and $3p$ orbitals have been excluded from the present calculations and the M shell has been permitted to contribute with d orbitals only, the

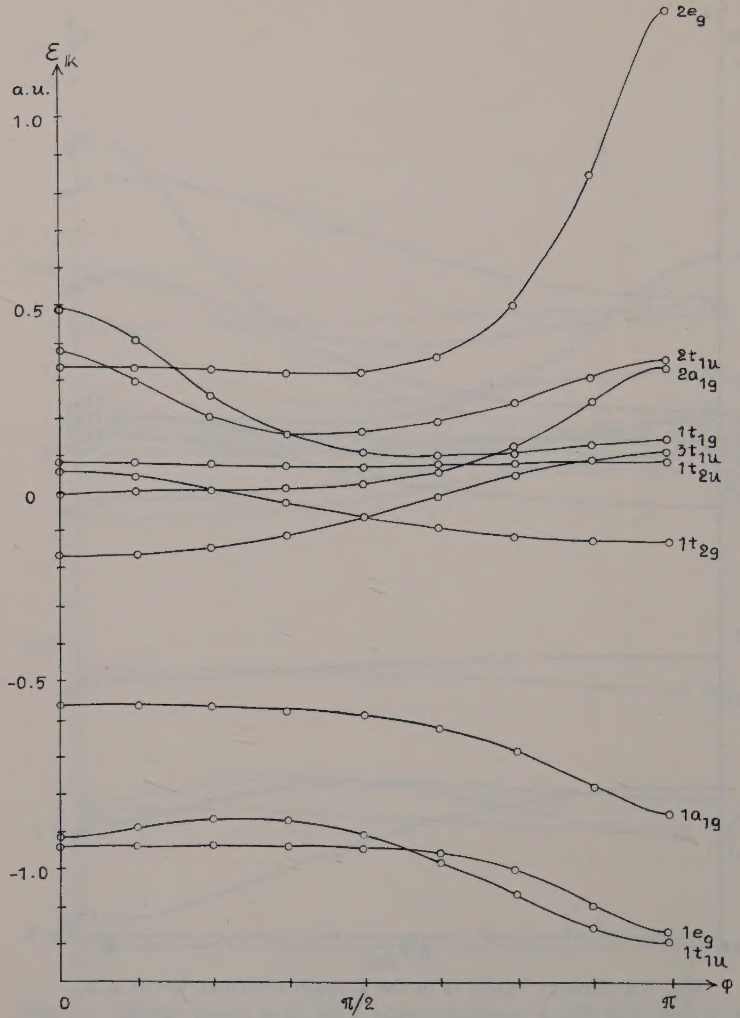

Fig. 2 e. Energy bands $\varepsilon_{\mathbf{k}}$ in the L approximation. $\mathbf{k} = (\varphi, \varphi, \varphi)$.

symmetry of which is very important on account of the point group symmetry of the crystal.

Five different choices for the effective charge, $Z = 1$, 2, 3, 4 and 5 have been made for the d orbitals in the present investigation. The modification of the d orbital exponents makes it necessary to use also modified effective charges for those integrals of type (19) and (20) of the effective Hamiltonian operator, containing d orbitals. The calculation of these new effective charges has been made according to the equations (49)–(53) occurring in [1]. Thus [1], Table 6 can be widened for the effective charges Z_0 of the diagonal one-centre energy integrals containing $3d$ orbitals. For the case $\lambda = 1$, the result is given by Table 1 for different d orbital exponents $Z/3$ ($Z = 1, \ldots 5$).

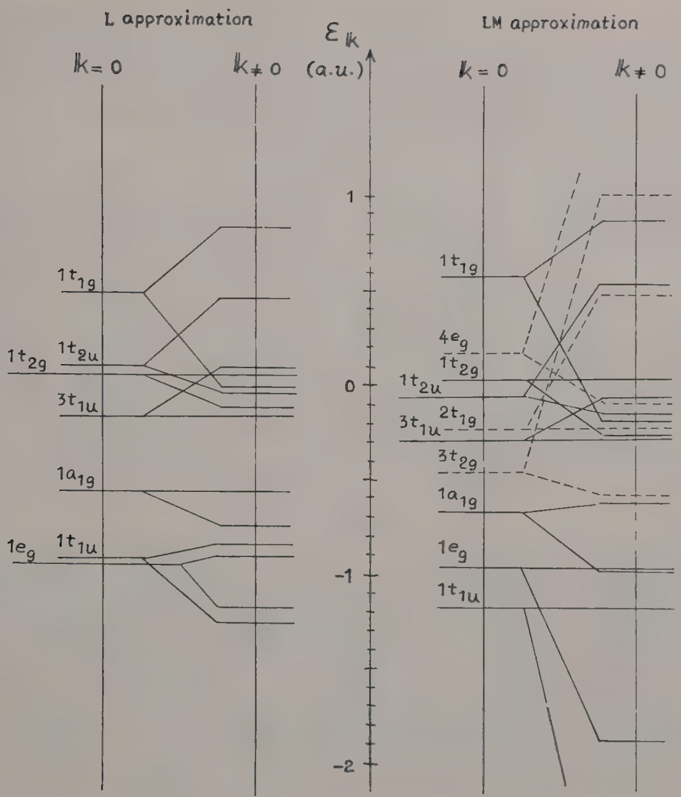

Fig. 3. Regions of the energy bands ε_k for the bonding and conducting orbitals in the L and LM approximations. Dotted lines correspond to rather uncertain LM bands not occurring in the L approximation.

Table 1. Effective charge, Z_0, for the diagonal one-centre integrals as a function of the d orbital exponent $Z/3$.

Z	1	2	3	4	5
Z_0	0.6700	0.7158	0.8213	0.9697	1.1317

As we see from Table 1, Z_0 for $3d$ orbitals with $Z=5$ is closest to the corresponding values for $2s$ and $2p$ (1.3540 and 1.2607, resp.), which is quite reasonable.

Considering the Z dependence for diagonal $3d$ integrals of (19), which are independent of the different types of $3d$ orbitals, we find a descending curve, mainly on account of the increase of Z_0. The most essential contribution, however, comes from the two-centre terms (20). It is found that the secular elements are rather considerably affected by the variation of Z. Certainly, the variation interval should be chosen much narrower to make it possible to draw reliable diagrams, but since a very great part of the calculations must be performed by use of desk machines, the time required to make these calculations would be quite long.

Table 2. Energy eigenvalues of the effective Hamiltonian operator (13) in a.u. for the occupied symmetry adapted orbitals in the L approximation (first line) and in the LM approximation (the following lines) given for different points in the wave vector space. On account of some indefinite overlap matrices several values have been omitted or put within parentheses.

Wave vector → Site orb.	Approx.	(0, 0, 0)	$\left(\frac{\pi}{2}\, 0, 0\right)$	(π, 0, 0)	$\left(0, \frac{\pi}{2}, 0\right)$ $\left(0, 0, \frac{\pi}{2}\right)$	(0, π, 0) (0, 0, π)	$\left(\frac{\pi}{2}, \frac{\pi}{2}, 0\right)$ $\left(\frac{\pi}{2}, 0, \frac{\pi}{2}\right)$	(π, π, 0) (π, 0, π)	$\left(0, \frac{\pi}{2}, \frac{\pi}{2}\right)$	(0, π, π)	$(\frac{\pi}{2}, \frac{\pi}{2}, \frac{\pi}{2}$
$1t_{1u}$	L	−0.916	−0.850	−0.923	−0.957	−1.017	−0.878	−1.009	−1.014	−1.255	−0.91
	$LM\ Z=1$	−1.072	−1.143	−2.762	−0.980		−0.991				−0.96
	2	(−1.576)									
	3					(−2.017)		(−3.939)		−1.765	−3.03
	4	−1.869	−1.514	−2.955	−1.874	−1.972	−1.727	(−3.814)	−1.940	−3.163	−2.14
	5	−1.211	−1.215	−1.743	−1.316			−2.803	−1.470	−2.282	−1.47
$1e_g$	L	−0.939	−0.992	−1.070	−0.917	−0.899	−0.965	−1.003	−0.902	−1.007	−0.94
	$LM\ Z=1$					−1.681	−1.177				−0.95
	2					(−2.466)					−1.22
	3	(−0.956)						−1.647	−1.892		(−1.67
	4	(−2.330)	(−1.656)	(−1.274)	−2.105	−1.345		−1.766	−1.456	−1.753	−1.67
	5	−1.370	−1.583	−2.026	−1.227	−1.132	−1.370	−1.412		−1.355	−1.26
$1a_{1g}$	L	−0.566	−0.572	−0.583	−0.572	−0.583	−0.582	−0.628	−0.582	−0.628	−0.59
	$LM\ Z=1$	−0.646	−0.627	−0.607	−0.627	−0.607	−0.621	(−0.628)	−0.621	(−0.628)	−0.63
	2	−0.714	−0.714	−0.820	−0.714	−0.820		(−0.657)		(−0.657)	
	3	−0.659	−0.642	−0.628	−0.642	−0.628	−0.626	−0.629	−0.626	−0.629	−0.61
	4		−0.592	−0.592	−0.592	−0.592	−0.592		−0.592		−0.60
	5	−0.575	−0.578	−0.585	−0.578	−0.585	−0.585	−0.629	−0.585	−0.629	−0.59
$3t_{1u}$	L	−0.166	−0.137	−0.086	−0.141	−0.102	−0.109	−0.012	−0.107	0.031	−0.07
	$LM\ Z=1$	−0.167	−0.140	−0.091	−0.141		−0.111	(−0.024)			−0.07
	2	(−0.280)	(−0.222)			−0.146		(−0.104)			(−0.16
	3	(−0.296)	(−0.185)			−0.199			(−0.230)		−0.12
	4	−0.220	−0.148	−0.088	−0.185	−0.138	−0.119	−0.034	−0.144	0.014	−0.08
	5	−0.179	−0.140	−0.086	−0.151			−0.016	−0.115	0.027	−0.07
$1t_{2g}$	L	0.058	0.066	0.075	−0.015	−0.061	−0.010	−0.053	−0.073	−0.142	−0.06
	$LM\ Z=1$	(0.055)	0.065	(0.075)		(−0.068)		(−0.071)	(−0.076)	−0.144	−0.07
	2									−0.208	−0.07
	3	(0.012)	(−0.110)	(−0.107)	−0.170	(−0.067)	−0.266		(−0.256)		−0.21
	4		−0.023	−0.009	−0.073	−0.094	−0.069	−0.093		−0.158	−0.10
	5	0.031	0.040	0.051	−0.042	−0.080	−0.036	−0.073	−0.094	−0.152	−0.09
$2t_{1g}$	$LM\ Z=1$	0.268	(0.221)	(0.113)	0.154	0.075	(0.905)	(0.288)	0.120	0.180	
	2	(−0.341)	(−0.120)	(−0.068)	−0.238	0.041	(−0.109)	(0.147)	−0.049	−0.041	−0.10
	3	(−0.222)	(−0.129)	(−0.079)	0.222	0.236		(0.887)	0.246	0.400	0.31
	4		(2.482)	(2.030)	0.737	0.546	0.936	0.737	0.597	0.575	0.66
	5	3.176	3.539	4.438	1.618	1.198	1.771	1.378	1.267	1.021	1.36
$1t_{1g}$	L	0.492	0.629	0.816	0.128	−0.002	0.169	0.042	0.074	0.074	0.10
	$LM\ Z=1$		(0.558)	(0.758)	0.115	−0.003	(0.159)	(0.040)	0.073	0.067	0.10
	2	(0.500)	(0.635)	(0.820)		−0.040	(0.144)	(0.019)			
	3	(0.584)	(0.702)	(0.875)	0.029	−0.086	0.157	0.003	−0.078	−0.152	−0.04
	4				0.066	−0.101	0.130	−0.028	−0.047	−0.160	−0.00
	5	0.477	0.626	0.814	0.104	−0.046	0.153	0.010	0.030	−0.012	0.06

Table 2 (continued).

ector →	$(0, 0, 0)$	$\left(\frac{\pi}{2} 0, 0\right)$	$(\pi, 0, 0)$	$\left(0, \frac{\pi}{2}, 0\right)$	$(0, \pi, 0)$	$\left(\frac{\pi}{2}, \frac{\pi}{2}, 0\right)$	$(\pi, \pi, 0)$	$\left(0, \frac{\pi}{2}, \frac{\pi}{2}\right)$	$(0, \pi, \pi)$	$\left(\frac{\pi}{2}, \frac{\pi}{2}, \frac{\pi}{2}\right)$	(π, π, π)
Approx.				$\left(0, 0, \frac{\pi}{2}\right)$	$(0, 0, \pi)$	$\left(\frac{\pi}{2}, 0, \frac{\pi}{2}\right)$	$(\pi, 0. \pi)$				
L	0.082	0.017	−0.032	0.108	0.143	0.031	−0.016	0.164	0.452	0.064	0.075
M $Z=1$	0.062	0.013	−0.034	0.089		0.028	(−0.023)	0.147	(0.413)	0.060	(0.059)
2	(0.042)								(0.431)		
3	(−0.051)	−0.052				−0.071	−0.137		(0.536)	−0.095	(−0.126)
4	0.030	−0.031	−0.091	0.058	0.083	−0.019	−0.085	0.115	(0.442)	0.009	−0.049
5	0.073	0.008	−0.046	0.096	0.125	0.019	−0.038	0.148	0.441	0.049	0.033
M $Z=1$	(0.203)	0.673		(0.304)	(0.442)	3.074	(0.355)	(0.966)	−0.017		0.163
2	(−0.149)	(−0.183)	(−0.181)	(−0.096)		(−0.376)			−0.092		−0.088
3	(−0.462)	(−0.601)	(−0.362)	−0.021	(0.005)	−0.086		(0.122)	0.050	−0.008	−0.009
4		0.431			0.634	0.548	0.309		0.371	0.452	0.665
5	0.864	1.028	1.295	0.818	0.793	0.945	1.245	0.773	0.724	0.872	0.903

Table 3. Coefficients occurring in the crystal orbitals of the occupied energy bands for the atomic orbital parts of the octahedral site orbitals given by Fig. 4 as functions of the wave vector. The coefficients are given in the *L* approximation and in the *LM* approximation for $Z=3$ for a few wave vectors.

ector	$(0, 0, 0)$		$(\pi, 0, 0)$		$(0, \pi, 0)$ $(0, 0, \pi)$		$(\pi, \pi, 0)$ $(\pi, 0, \pi)$		$(0, \pi, \pi)$		(π, π, π)	
nation	*L*	*LM*	*L*	*LM*	*L*	*LM*	*L*	*LM*	*L*	*LM*	*L*	*LM*
bital												
s	0.981	0.932	0.925	0.847	0.976	0.912	0.908	0.930	0.965	0.936	0.880	0.827
$p\sigma$	0.109	−0.030	−0.273	−0.219	0.096	0.097	−0.296	0.014	0.065	0.120	−0.327	0.138
$p\pi$	−0.161	0.034	−0.263	−0.002	−0.195	0.129	−0.297	−0.355	−0.254	−0.003	−0.344	0.395
$d\sigma$		0.325		0.343		0.328		0.087		−0.215		−0.028
$d\pi$		0.153		0.342		0.187		0.049		0.251		0.375
s	0.933	0.694	0.921	0.977	0.949	0.961	0.939	0.957	1.000	0.995	1.000	0.996
$p\sigma$	−0.361	0.413	−0.388	−0.038	−0.315	−0.248	−0.343	−0.113	−0.011	−0.042	−0.020	0.059
$d\sigma$		−0.561		−0.033		0.041		−0.245		0.071		0.013
$d\delta$		−0.180		−0.209		−0.118		−0.104		−0.054		−0.066
s	0.989	0.916	0.974	0.948	0.974	0.948	0.948	0.954	0.948	0.954	0.893	0.853
$p\sigma$	0.146	−0.160	0.227	−0.012	0.227	−0.012	0.320	0.295	0.320	0.295	0.450	0.497
$d\sigma$		−0.367		−0.317		−0.317		−0.044		−0.044		0.160
s	−0.405	−0.209	−0.693	−0.468	−0.407	−0.315	−0.482	0.850	−0.691	−0.168	−0.601	−0.307
$p\sigma$	0.532	0.479	0.333	−0.306	0.531	0.410	0.460	−0.301	0.254	0.438	0.339	−0.176
$p\pi$	0.743	0.691	0.640	0.679	0.743	0.731	0.746	0.120	0.677	0.786	0.724	0.789
$d\sigma$		0.497		0.458		0.444		−0.049		0.117		0.411
$d\pi$		−0.055		0.133		−0.016		0.412		0.386		0.289
$p\pi$	1.000	0.037	1.000	0.703	1.000	0.828	1.000	0.155	1.000	0.743	1.000	0.624
$d\pi$		−0.761		0.412		0.467		0.405		0.116		−0.015
$d\delta$		0.647		0.579		−0.311		−0.901		0.659		0.781

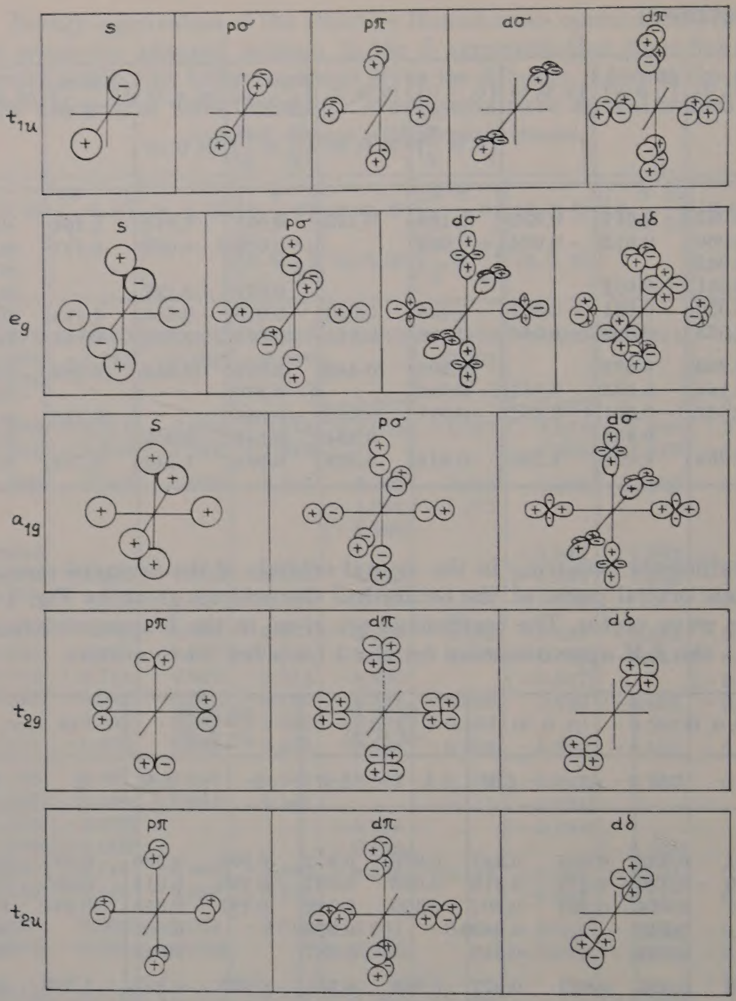

Fig. 4. Symmetry shapes for the atomic orbital parts of the occupied symmetry adapted octahedral site orbitals.

As is seen from Table 2 and Fig. 1, the energy bands found by solving the different secular equations corresponding to [1], section 3, are lowest in general for $Z=3$, but this minimum value varies between $Z=2$ and 4 for different orbitals and different wave vectors. For the Z values minimizing the energy the interaction range of the corresponding orbitals is, however, sufficiently large to give indefinite overlap matrices for many of the secular equations, though boron neighbours up to the fourth order of magnitude (24 nearest neighbours) have been taken into account. This is also the reason why many of the columns in Table 2 are incomplete. The numerical results obtained, however, give sufficient evidence for establishing the existence of minima for the orbital energies for Z

]

values lying between 2 and 4. Far from the minimum points it is found that the orbital energies tend asymptotically towards the L approximation.

The secular equations have been solved in general only for wave vectors with high symmetry in the reciprocal space. In the L approximation, however, the bands have been given for seven directions of high symmetry including many intermediate points (Figs. 2a–e), although the symmetry adapted orbitals are in fact somewhat mixed for these points. But, since this mixing enters only in the interaction integrals between neighbouring sites, it might be neglected. Fig. 3 gives a direct comparison between the regions of the energy bands in the L approximation and the LM approximation for the best choice of Z.

The atomic orbital parts of the different occupied symmetry adapted site orbitals are described in Fig. 4. The coefficients for these atomic orbital parts occurring in the hybridizations have been given for a few wave vector points in Table 3 for the different occupied symmetry adapted orbitals in the L and LM approximations.

3. Discussion of the results

The results given in the previous section show the importance of taking M shell orbitals into account. Though the sequences of all the common levels are generally equal in the L and LM approximations, the lowest lying orbital energies are essentially lowered, when $3d$ orbitals are taken into account. Strong indication was found for the supposition made in [1] that the crystal orbital exponents for the M shell electrons should be chosen much larger than for the free atom case. It is interesting that the most suitable Z values are so remarkably high (Table 2 and Fig. 1). This depends on the ligand field of the crystal. For similar reasons a small effect can probably be expected, also when the L shell crystal orbital exponents are varied. This fact remains to be investigated.

The energy bands in the L approximation, given by Fig. 2, can be compared to the energy bands given by Longuet-Higgins *et al.* [5], who consider the same case. The main difference is that Longuet-Higgins *et al.* have used several very rough approximations and assumptions in addition to those used here. These assumptions are as follows:

1. Two-centre energy integrals are supposed to be proportional to the corresponding overlap integrals.
2. $2s$ and $2p$ orbital integrals are supposed to be equal.
3. Only the first order of boron neighbours are considered.

On account of these approximate assumptions, one cannot expect the present results to be essentially in accordance with [5]. The main difference is that some of the present bands are conduction bands, while Longuet-Higgins *et al.* have found a complete shell description. Moreover, the sequences of the energy bands are somewhat different in the two investigations.

Fig. 3 is suitable for a comparison between the L approximation and the LM approximation. It is seen that the lowest lying levels are lowered, while the higher levels are further raised by the introduction of d orbitals. Both the approximations have the qualitative results in common, that there are completely occupied bonding orbital bands, $1t_{1u}$, $1e_g$ and $1a_{1g}$ and conduction bands, $3t_{1u}$, $1t_{2g}$, $1t_{2u}$ and $1t_{1g}$. In the LM approximation some new conduction bands also occur ($3t_{2g}$, $2t_{1g}$ and $4e_g$). These bands are, however, very wide and cannot be given with great accuracy, since they do not exist in the L approximation. The main difference from the results of [1] is the fact that there is a small finite gap between the fully occupied bands and the conduction bands (see Fig. 3).

The occupation numbers of the different bands can be roughly estimated by considering the number of calculated points of the energy bands with sufficiently low energy. A rough description of the configuration can be given by

$$(1\,t_{1u})^6\,(1\,e_g)^4\,(1\,a_{1g})^2\,(3\,t_{1u})^5\,(1\,t_{2g})^3. \tag{22}$$

Thus 12 valence electrons occupy a closed shell and the remaining 8 are conduction electrons moving throughout the whole crystal. A certain very small contribution may come, however, from the conduction bands $3t_{2g}$, $2t_{1g}$, $1t_{1g}$ and $1t_{2u}$. The orbitals $2a_{1g}$, $2t_{1u}$ and $2e_g$ occurring in both the L and LM approximations are antibonding. The results given above form very good verifications for the supposition that the crystal is ionized and for the conductivity of the bivalent metal borides of type MB_6.

The coefficients of the different atomic orbital parts given in Table 3 indicate a remarkably great contribution from the d orbitals, although the corresponding numerical values may not be considered as quite reliable, on account of the large d overlap. The qualitative results, however, are ascertained and the experimentally found stability and conductive properties of the CaB_6 crystal are satisfyingly verified.

For their support and kind interest I want to thank Professor O. Klein and Dr. I. Hjalmars. For free Besk time and also for sponsoring part of the additional numerical work I am very grateful to *Statens Naturvetenskapliga Forskningsråd.* For numerical calculations of the secular elements my thanks are due to Mr. N. B. Nilsson.

Institute of Theoretical Physics, University of Stockholm, January 1960.

REFERENCES

1. S. Flodmark, Ark. Fys. *14*, 513 (1959).
2. R. Kiessling, Acta Chem. Scand. *4*, 209 (1950).
3. S. Flodmark, Ark. Fys. *9*, 1357 (1955).
4. S. Flodmark, Svensk Kem. Tidskr. *70*, 521 (1958).
5. H. C. Longuet-Higgins and M. de V. Roberts, Proc. Roy. Soc. *A 224*, 336 (1954).
6. Handbuch der Physik VII, 1 p. 135. Springer-Verlag, Berlin-Göttingen-Heidelberg (1955).
7. S. Flodmark, Ark. Fys. *17*, 81 (1960).
8. S. Flodmark, Table of Molecular A and B Functions. Institute of Theoretical Physics, Stockholm (1957).
9. W. E. Duncanson and C. A. Coulson, Proc. Roy. Soc. Edinb. *A 62*, 37 (1943).

Tryckt den 2 augusti 1960

Uppsala 1960. Almqvist & Wiksells Boktryckeri AB